Supplemental Materials

Molecular Biology of the Cell

Patnaik et al.

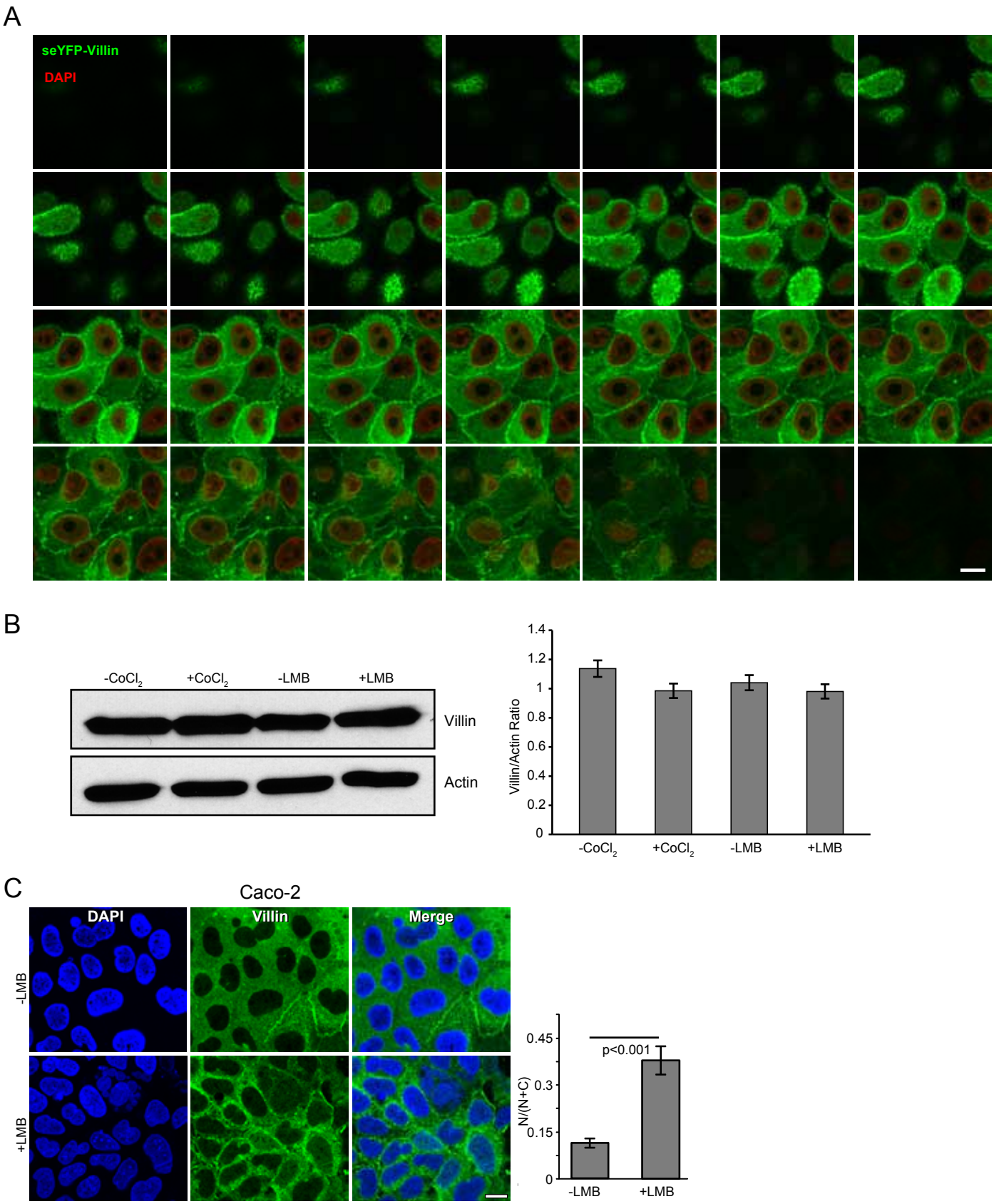

Supplementary Figure S1. (A) Confocal image showing individual z stacks from MDCK Tet-Off cells expressing seYFP-villin. Pseudo-red represents the nuclear dye DAPI (4',6'-diamidino-2-phenylindole) staining. Images were collected at 0.25 μm intervals. (B) Comparison of villin expression levels in the presence or absence of $CoCl_2$ (400μM) or leptomycin B (20nM) treatment with untreated seYFP tagged villin expressing MDCK cells. (C) Representative images of endogenous villin in Caco-2 cells treated with 20 nM leptomycin B (+LMB) or vehicle control (-LMB) for 8 h. LMB treatment increases nuclear villin accumulation compared to vehicle control. Nuclei was stained with DAPI.

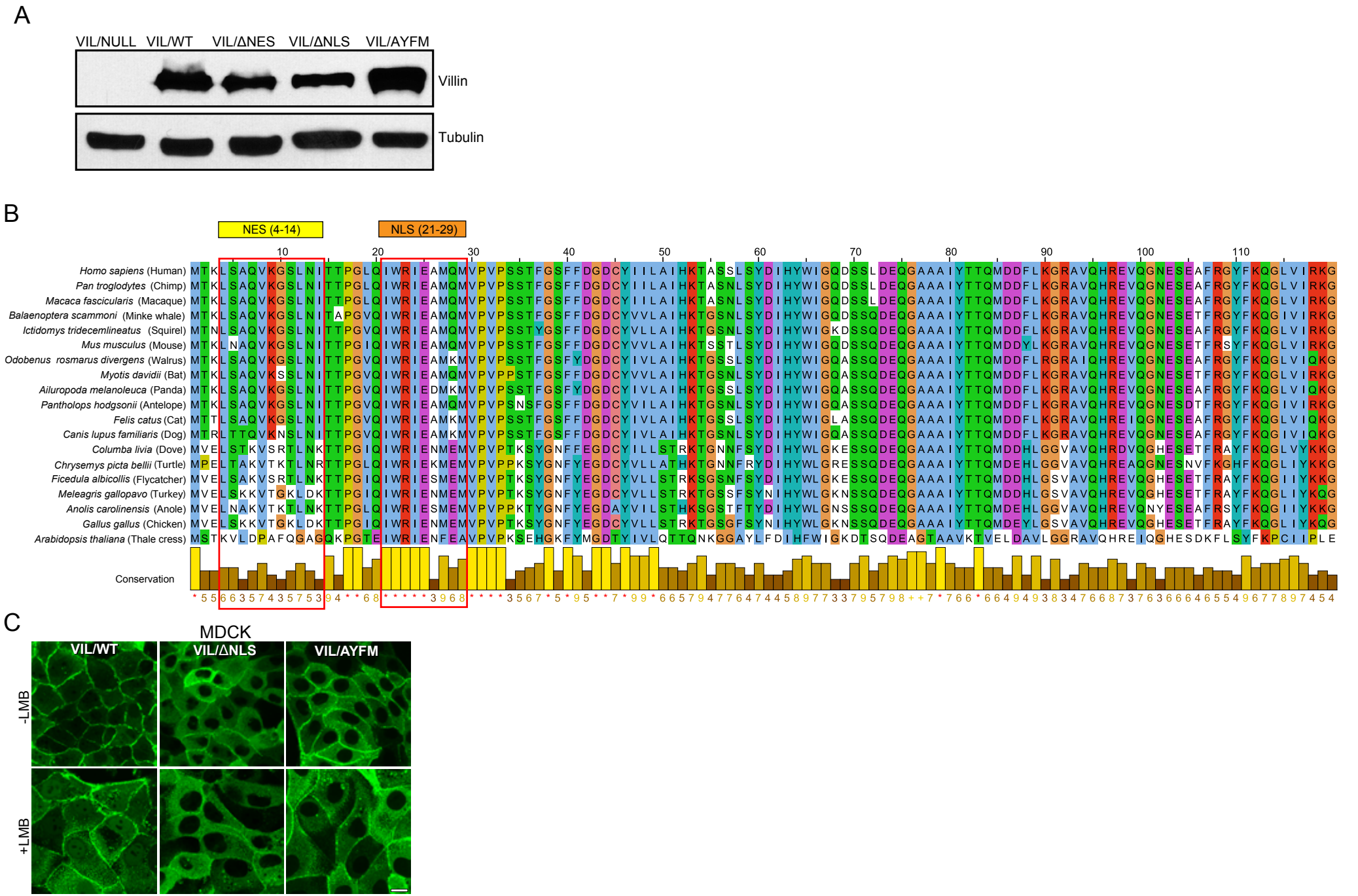

Supplementary Figure S2. (A) Expression of seYFP-tagged wild-type (VIL/WT) or mutant villin (VIL/ΔNLS; VIL/ΔNES; VIL/AYFM) in MDCK Tet-Off cells (VIL/NULL). (B) Schematic diagram showing sequence homology between human villin and villin from different species including mammals, reptiles and birds. Sequence conservation is shown at the bottom. (C) Representative images of seYFP-tagged villin, VIL/WT, VIL/ΔNLS and VIL/AYFM in cells treated with 20 nM leptomycin B (+LMB) or vehicle control (– LMB) for 8h. No nuclear villin was noted in VIL/ΔNLS and VIL/AYFM cells treated with LMB compared to VIL/WT cells.

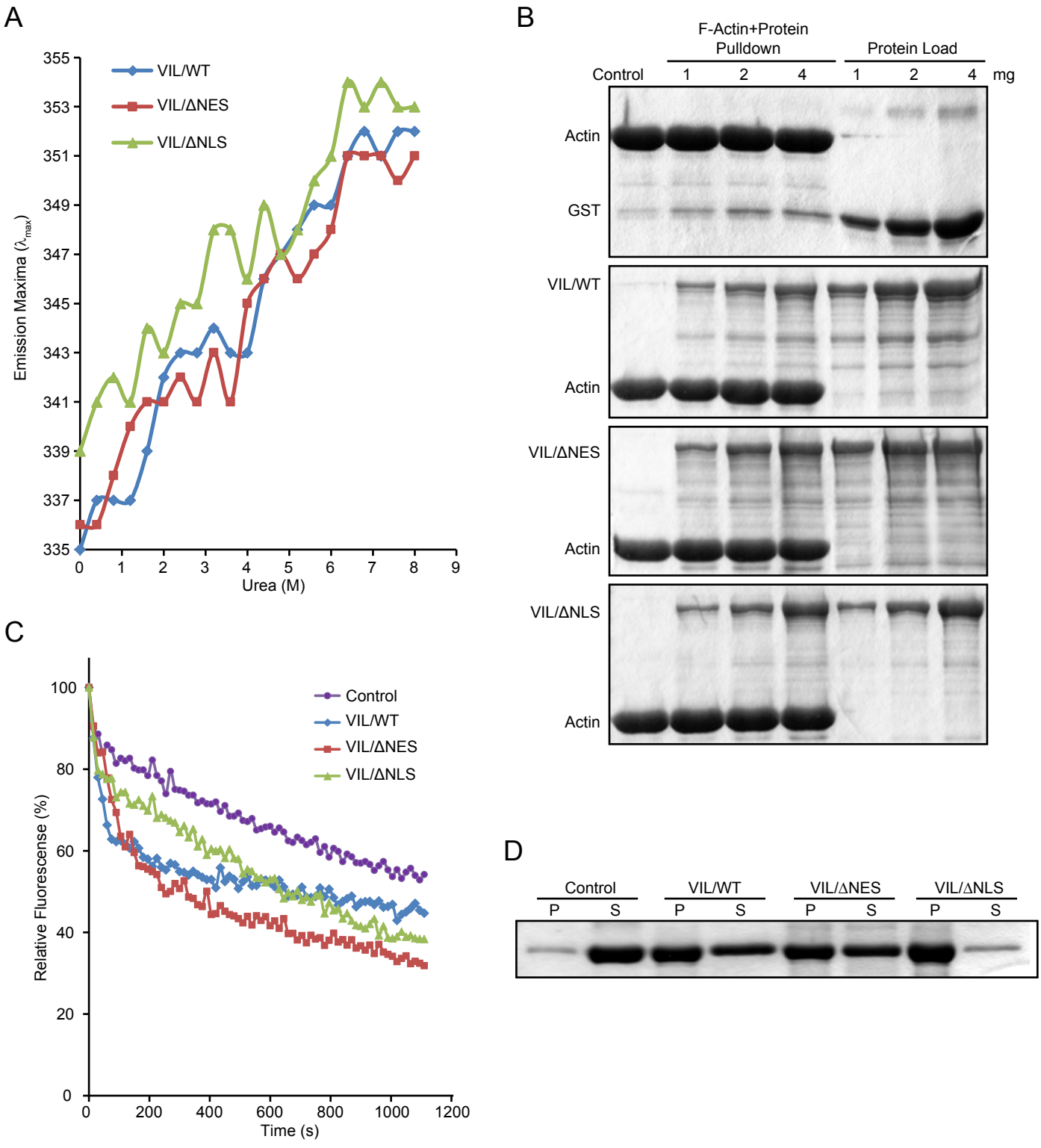

Supplementary Figure S3 Villin mutants VIL/ΔNES and VIL/ΔNLS retained their structure as well as activity when compared with wild type villin protein (VIL/WT) as determined by biochemical assays (A) Urea denaturation assay: Recombinant villin proteins (1μM) were incubated with increasing amounts of urea (0-8M) for 1h and the fluorescence was measured at excitation wavelength of 280nm and emission scan at 300nm-420nm using Floromax-4 fluorimeter. (B) Actin binding assay: F-Actin was incubated with increasing amounts (0-4mg) of GST control or GST-tagged VIL/WT, VIL/ΔNES and VIL/ΔNLS protein.(C) Severing activity of the proteins was compared by adding the proteins to pyrene labelled F-actin and measuring the loss of fluorescence using a Fluoromax-4 fluorimeter at excitation at 365nm and emission at 407nm over a period of 1100s. (D) Actin bundling activity was compared by incubating the proteins with F-actin for 1h at room temperature followed by low speed centrifugation at 10,000g for 15 minutes. Actin in the pellet (P) represents the bundled actin while the actin in the supernatant (S) represents the unbundled F-actin.

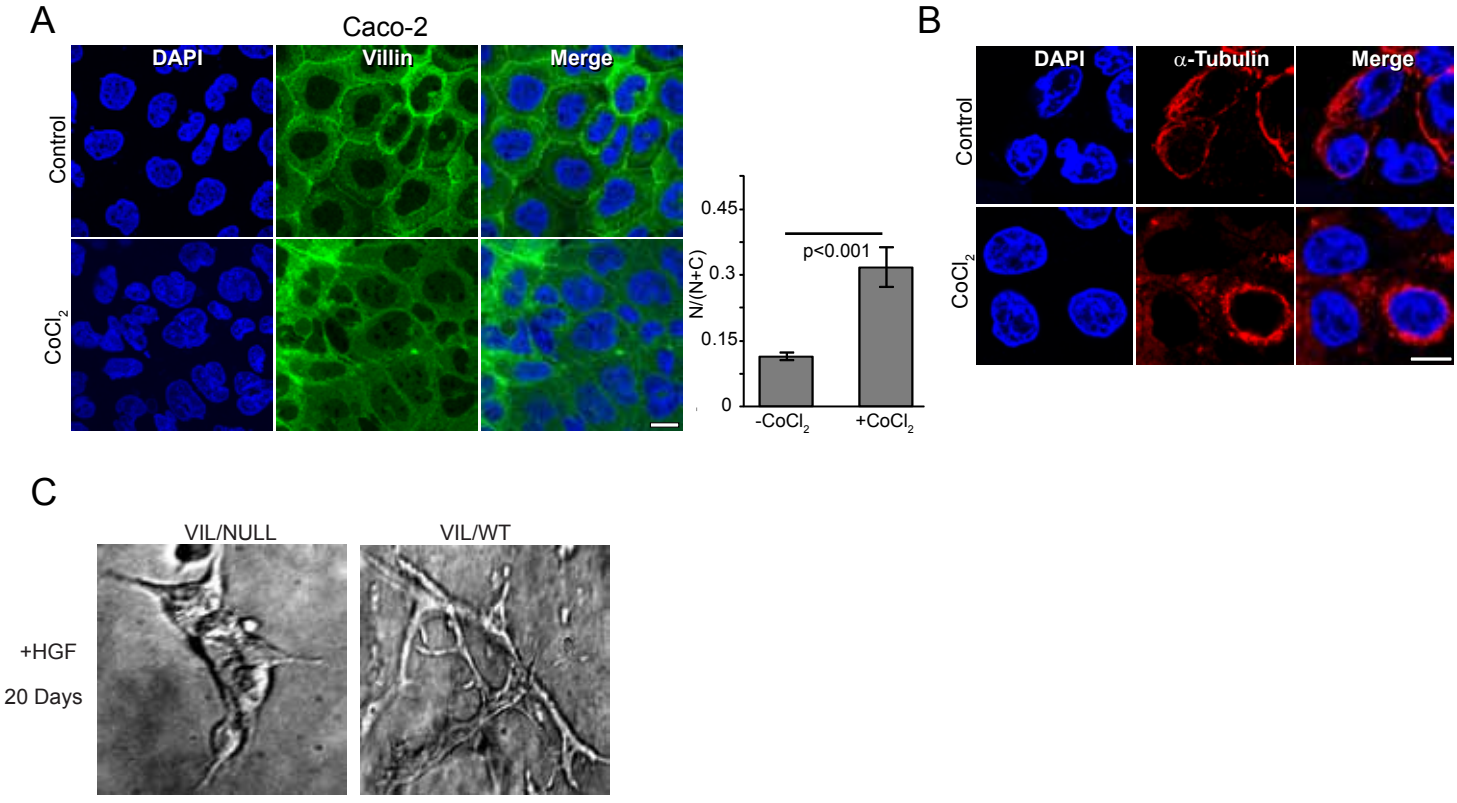

Supplementary Figure S4. (A) Representative images of endogenous villin in Caco-2 cells treated with 400 μM cobalt chloride ($CoCl_2$) or vehicle control for 8h. Bar, 5 μm. (B) Representative images of α-tubulin from MDCK cells expressing VIL/WT cells treated with 400 μM cobalt chloride ($CoCl_2$) or vehicle control for 8h. Bar, 5 μm. (C)Tubulogenesis of VIL/NULL and VIL/WT 20 days post-HGF treatment. Representative phase contrast image shows VIL/WT cells maintain morphogenesis of a well established tubule 20 days post-HGF treatment. This is a representative of six other experiments with similar results.

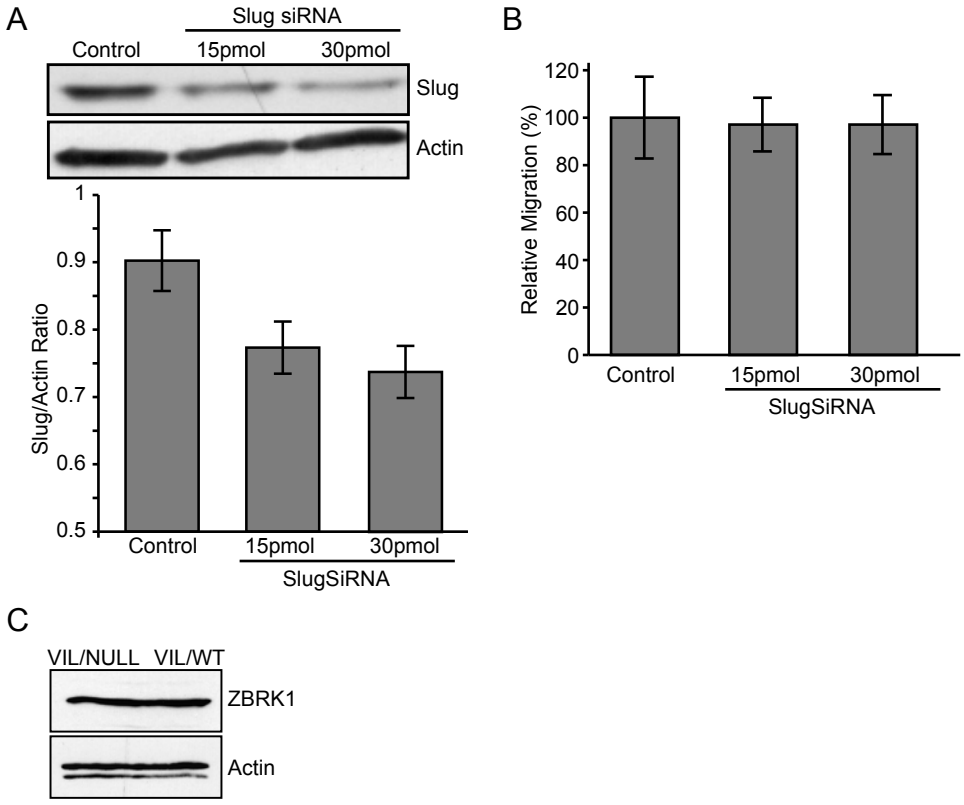

Supplementary Figure S5. (A) Knockdown of Slug using siRNA in MDCK Tet-Off cells. Actin was used as a loading control. (B) Cell migration was measured using a wound healing assay in MDCK cells with control siRNA or with Slug knocked down using siRNA. (C) Expression of endogenous ZBRK1 in MDCK VIL/NULL and VIL/WT expressing cells. Actin was detected as a loading control. Data is representative of three independent experiments.